

Nanotube-assisted protein deactivation

AMIT JOSHI¹, SUPRIYA PUNYANI¹, SHYAM SUNDHAR BALE¹, HOICHANG YANG²,
THEODORIAN BORCA-TASCIUC³ AND RAVI S. KANE^{1*}

¹The Howard P. Isermann Department of Chemical and Biological Engineering, Rensselaer Polytechnic Institute, Troy, New York 12180, USA

²Rensselaer Nanotechnology Center, Rensselaer Polytechnic Institute, Troy, New York 12180, USA

³Department of Mechanical, Aerospace, and Nuclear Engineering, Rensselaer Polytechnic Institute, Troy, New York 12180, USA

*e-mail: kaner@rpi.edu

Published online: 9 December 2007; doi:10.1038/nnano.2007.386

Conjugating proteins onto carbon nanotubes has numerous applications in biosensing^{1,2}, imaging and cellular delivery^{3–5}. However, remotely controlling the activity of proteins in these conjugates has never been demonstrated. Here we show that upon near-infrared irradiation, carbon nanotubes mediate the selective deactivation of proteins *in situ* by photochemical effects. We designed nanotube–peptide conjugates to selectively destroy the anthrax toxin, and also optically transparent coatings that can self-clean following either visible or near-infrared irradiation. Nanotube-assisted protein deactivation may be broadly applicable to the selective destruction of pathogens and cells, and will have applications ranging from antifouling coatings to functional proteomics.

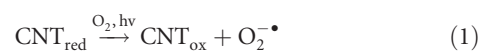
Biological systems are relatively transparent at near-infrared (NIR) wavelengths (700–1,100 nm), so we tested whether the ability of carbon nanotubes to absorb NIR radiation (Fig. 1a) could provide control over the activity of adsorbed proteins. The localized generation of heat resulting from the NIR irradiation of nanomaterials such as nanoshells and carbon nanotubes has previously been used to effect cell death^{4–6}. In principle, such a photothermal effect might also influence the activity of proteins adsorbed onto carbon nanotubes. The irradiation of nanotubes might also influence the activity of adsorbed proteins photochemically. The irradiation of complexes formed by DNA-wrapped single-walled carbon nanotubes (SWNTs) and silver ions results in the reduction of silver ions to silver⁷, and the irradiation of other nanomaterials such as fullerenes and quantum dots^{8–11} can result in the generation of reactive oxygen species (ROS). If reactive species are generated upon irradiation of nanotubes, these species might influence the activity of adsorbed proteins.

For initial experiments, we adsorbed the enzyme alcohol dehydrogenase (ADH) onto SWNTs (Thomas Swan & Co.) from aqueous buffer (see Methods). NIR irradiation by a continuous wave laser resulted in a significant loss of enzymatic activity of SWNT–ADH conjugates (Fig. 1b). In contrast, NIR irradiation of a solution of ADH did not result in a loss of activity (Fig. 1b). Interestingly, SWNT–ADH conjugates showed negligible loss of activity over 60 min at 60 °C (Fig. 1b). However, for the concentrations of SWNT–ADH conjugates used for these experiments, NIR irradiation of a solution initially at room temperature (~23 °C) resulted in an increase in the global temperature of only 8 °C over 60 min (Fig. 1c). Theoretical work by Keblinski *et al.*¹² indicates that the local temperature rise adjacent to an SWNT following heating by a continuous wave laser would be negligible, and that the heating would be homogeneous

over large volumes. Consistent with these predictions, a Raman spectroscopy-based measurement of local nanotube temperature indicated a negligible change in temperature following irradiation of SWNT films covered with a layer of water (see Supplementary Information, Fig. S1). Collectively, these results indicate that a photothermal effect—previously used for NIR-mediated cell killing by nanomaterials—is not the basis of the reported NIR-induced protein deactivation (Fig. 1b).

We next tested whether protein deactivation was mediated by the photoinduced generation of free radicals. Bubbling argon gas through the sample to decrease the amount of dissolved oxygen significantly inhibited SWNT–ADH deactivation (Fig. 2a), suggesting a role for photogenerated ROS. Furthermore, protein deactivation was inhibited by 2 mM disodium terephthalate (a hydroxyl radical quencher), 200 μM superoxide dismutase-mimetic Mn-TBAP, and 200 mM mannitol (a quencher of both hydroxyl radicals and superoxide anions¹³). However, little inhibition of deactivation was observed in the presence of sodium azide, a quencher of singlet oxygen, at concentrations as high as 200 mM. Similar results were obtained for conjugates of ADH with ‘super-purified HiPco’ SWNTs (Carbon Nanotechnologies; see Supplementary Information, Fig. S2), conjugates of SWNTs with the protease Subtilisin Carlsberg (SC) (Fig. 2b), and conjugates of multiwalled carbon nanotubes (MWNTs) with ADH (Fig. 2c). Collectively, these results suggest that the nanotube-assisted protein deactivation is mediated primarily by generated ROS—specifically hydroxyl radicals and superoxide anions. These ROS are known to cause protein fragmentation and amino-acid modification¹⁴. We further validated the proposed photochemical mechanism by confirming the generation of superoxide anions and hydroxyl radicals following NIR irradiation of nanotubes (see Supplementary Information, Fig. S3).

Based on these results, we propose the following model for the photoinduced nanotube-assisted ROS generation:



Optical excitation and subsequent electron transfer to oxygen results in the formation of a superoxide anion and an oxidized carbon nanotube (CNT_{ox}); a similar electron-transfer-based

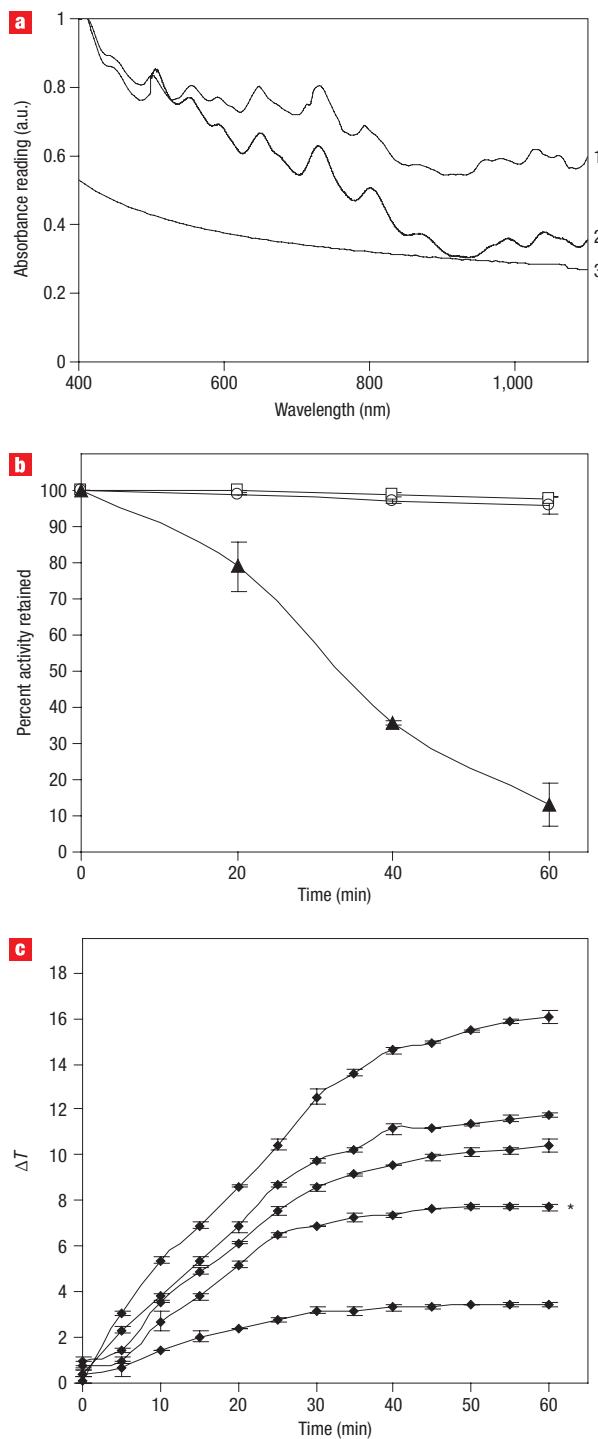


Figure 1 Behaviour of nanotube and nanotube-protein conjugates after NIR irradiation. **a**, Visible-NIR absorption spectrum of (1) surfactant-solubilized 'super-purified' HiPco SWNTs, (2) surfactant-solubilized SWNTs and (3) oxidized MWNTs. **b**, Protein activity of SWNT-ADH conjugates (filled triangles) and native ADH (open squares) upon NIR irradiation at room temperature, and SWNT-ADH conjugates at 60 °C in the absence of NIR irradiation (open circles). **c**, Irradiating a solution of SWNT-ADH with NIR at room temperature (~23 °C) results in global heating. The change in temperature (ΔT) is shown for SWNT concentrations of 1, 0.5, 0.2 and 0.1 mg ml⁻¹ (from top to bottom), and without SWNTs (the bottom-most curve). The asterisk indicates the data for SWNT concentrations used for the NIR irradiation experiments. Error bars represent the standard deviations from triplicate measurements.

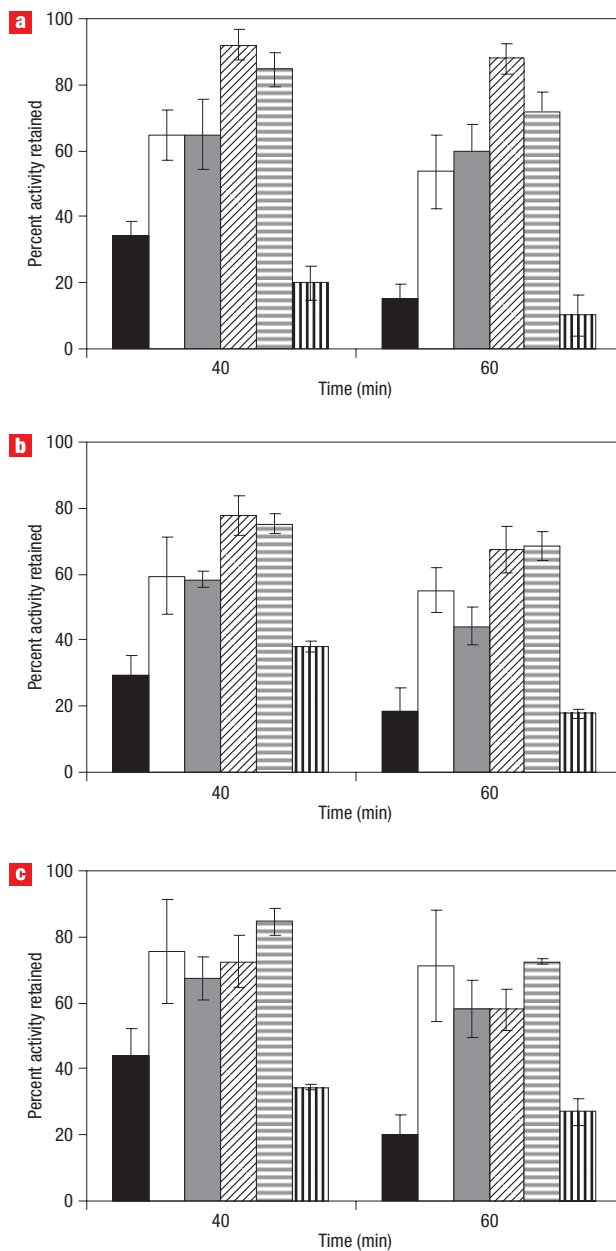
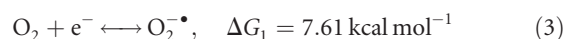


Figure 2 Deactivation behaviour of nanotube-protein conjugates. Extent of protein deactivation after 40 min and 60 min for SWNT-ADH (**a**), SWNT-SC (**b**) and MWNT-ADH (**c**) conjugates in the absence of quenchers (black), after bubbling with argon (white), and in the presence of 2 mM disodium terephthalate (grey), 200 μ M Mn-TBAP (diagonal stripes), 200 mM mannitol (horizontal stripes) and 200 mM sodium azide (vertical stripes). Error bars represent standard deviations from triplicate measurements.

mechanism has been proposed for superoxide anion generation following the irradiation of TiO₂ (ref. 15). The adsorption of oxygen onto nanotubes in aqueous solution^{16,17} may facilitate the proposed electron transfer (equation 1).

Analysis of the electron-transfer thermodynamics² suggests that this proposed mechanism is plausible. For the O₂/O₂⁻ redox pair, the half potential (compared with a normal hydrogen electrode, NHE) is -0.33 V (ref. 18):



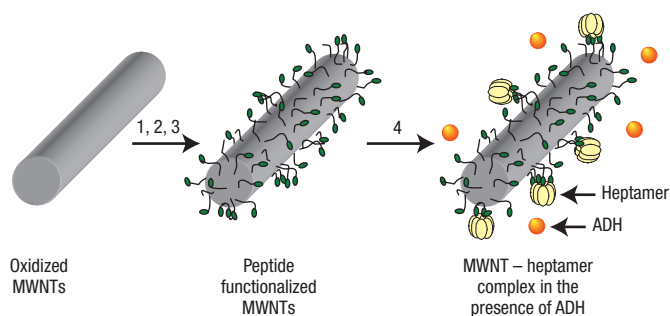
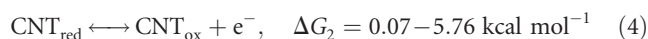


Figure 3 Functionalizing carbon nanotubes with peptides that recognize anthrax toxin. Oxidized MWNT is treated with (1) mono-N-t-boc-amido-dPEG₁₁-amine, (2) chloroacetic anhydride and (3) peptide (Ac-HTSTYWLDGAPC-amide) that binds to the heptamer, [PA₆₃]₇, in anthrax toxin, and subsequently added to a mixture of heptamer and ADH (4).

Similarly, the potential E_{SWNT} (versus NHE) for the one electron withdrawal from a nanotube ranges from -0.25 to -0.003 V for semiconducting nanotubes^{2,19}:

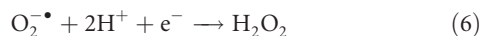


The free energy change for the withdrawal of an electron from the nanotube surface by an oxygen molecule (equation 1) therefore ranges from 7.68 to 13.37 kcal mol⁻¹:

$$\Delta G = \Delta G_1 + \Delta G_2 = 7.68 - 13.37 \text{ kcal mol}^{-1} \quad (5)$$

For irradiation at 975.5 nm, the energy of the incident photons (~ 1.26 eV per photon or 29.17 kcal mol⁻¹) would therefore be sufficient to induce this electron transfer.

Reduction of the oxidized carbon nanotube by water or hydroxide ions would complete the cycle^{7,20}. Hydroxyl radicals may be generated from water or hydroxide ions during this process (equation 2), or possibly from photogenerated superoxide anions by means of the following series of reactions^{15,18}:



The half potentials (versus NHE) for the $\text{O}_2^{\bullet -}/\text{H}_2\text{O}_2$ and $\text{H}_2\text{O}_2/\text{OH}^{\bullet}$ redox pairs are 0.94 V and 0.46 V, respectively¹⁸, and these reactions are feasible.

The unique properties of carbon nanotubes enable nanotube-assisted protein deactivation to be exploited in several contexts. Our first demonstration uses polyvalent interactions. We reasoned that polyvalent carbon nanotubes^{21,22}, presenting multiple copies of a suitable ligand, could be used for the selective high-affinity binding and NIR radiation-assisted destruction of anthrax toxin (Fig. 3). It is the anthrax toxin that is responsible for the major symptoms and death in anthrax. We therefore functionalized MWNTs with the peptide HTSTYWLDGAPC, which binds to the heptameric receptor-binding subunit of anthrax toxin ([PA₆₃]₇) (ref. 23). Peptide-functionalized MWNTs were added to a solution containing a 1:1 mixture of [PA₆₃]₇ and ADH, exposed to NIR radiation, and the amount of PA₆₃ and ADH was characterized using SDS-polyacrylamide gel electrophoresis

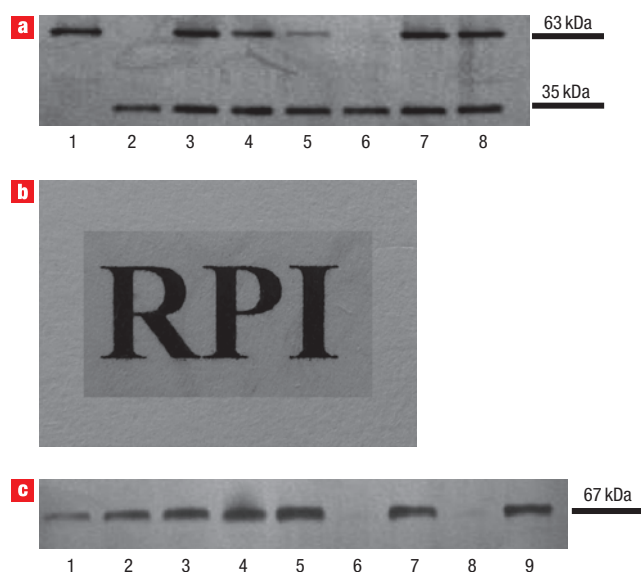


Figure 4 Applications of nanotube-assisted protein deactivation.

a, Peptide-functionalized MWNTs in selective destruction of anthrax toxin. SDS-PAGE of heptamer [PA₆₃]₇ (lane 1); ADH (lane 2); a mixture of MWNT-peptide conjugates, [PA₆₃]₇ and ADH exposed to NIR radiation for 0 min (lane 3), 40 min (lane 4), 80 min (lane 5), 120 min (lane 6) and 120 min with mannitol (lane 7); and a mixture of control thioglycerol-functionalized MWNTs, [PA₆₃]₇ and ADH exposed to NIR radiation for 120 min (lane 8). **b**, Optical micrograph of a transparent nanotube film. Text lies beneath the film. **c**, Transparent nanotube films are self-cleaning after NIR or visible irradiation. SDS-PAGE shows BSA at 10, 20, 50 and 100 ng (lanes 1–4); residual protein adsorbed onto nanotube film after incubation with 1 mg ml⁻¹ BSA for 30 min and exposure to neither NIR nor visible radiation (lane 5), NIR radiation for 4 h in the absence (lane 6) and presence (lane 7) of mannitol; exposure to visible light for 2 h in the absence (lane 8) and presence (lane 9) of mannitol.

(SDS-PAGE). The amount of PA₆₃ decreased with increasing time of NIR exposure, but no significant change was seen in the amount of ADH (lanes 3–6, Fig. 4a), indicating the selective destruction of the target protein. Little or no decrease in the amount of PA₆₃ or ADH was seen for samples irradiated in the presence of mannitol (lane 7) or using control thioglycerol-functionalized MWNTs (lane 8). This selective destruction strategy should be broadly applicable for the neutralization of pathogens and toxins *in vitro* (for example, for the decontamination of biopharmaceuticals or of blood during haemodialysis) and potentially even *in vivo*. Selective protein deactivation may also be useful in functional proteomics, by helping elucidate protein function.

We also exploited the photoinduced ROS generation in conjunction with the ability of nanotubes to form ultrathin, flexible and transparent films²⁴ to fabricate self-cleaning²⁵ films (for example, films that eliminate protein fouling). Protein fouling is a significant problem, as it can mediate bacterial attachment to surfaces and biofilm formation. We fabricated optically transparent nanotube films (Fig. 4b) (see Methods), exposed them to a 1 mg ml⁻¹ solution of bovine serum albumin (BSA), and then to NIR radiation. As seen in Fig. 4c, NIR irradiation resulted in removal of adsorbed protein (lane 6). Similar self-cleaning properties were observed (lane 8) following exposure to visible light from a fluorescent bulb whose output spectrum mimics daylight (see Methods). No significant decrease

in the extent of protein adsorption was observed in the presence of mannitol following either NIR (lane 7) or visible (lane 9) irradiation. Characterization by X-ray photoelectron spectroscopy, transmission electron microscopy and experiments using C^{14} -labelled BSA confirmed the ability to remove adsorbed protein from the films by irradiation (see Supplementary Information, Figs S4, S5 and S6, respectively). Similar self-cleaning behaviour was observed *in situ* when the nanotube film was exposed to a solution of BSA in the presence of light from a fluorescent bulb (see Supplementary Information, Fig. S7). Nanotube-assisted free radical generation should represent a general strategy to eliminate surface fouling.

In summary, this study provides mechanistic insight into an interesting new phenomenon—nanotube-assisted protein deactivation. The unique properties of carbon nanotubes facilitate applications of this phenomenon. In particular, nanotubes serve as attractive scaffolds for the polyvalent display of ligands, thereby enabling them to recognize pathogens or cells selectively and with high affinity. The approach that we have applied for the selective degradation of a component of anthrax toxin may be broadly applicable for the targeted destruction of a variety of pathogens and toxins. The nanotube-mediated generation of ROS following NIR irradiation may also represent an exciting approach for the targeted destruction of cells (for example, tumour cells), which is complementary to previously reported photothermal approaches⁴. Furthermore, the ability to generate stable ultrathin nanotube coatings that are optically transparent and self-clean on exposure to even visible light would be particularly advantageous for numerous indoor and outdoor applications. Nanotube-assisted deactivation therefore represents a general and facile strategy for the targeted destruction of proteins, pathogens and cells, with applications ranging from antifouling coatings to proteomics and novel therapeutics.

METHODS

FUNCTIONALIZING NANOTUBES

Enzymes were adsorbed onto SWNTs (Elicarb SW, Thomas Swan & Co.) as described previously²⁶. To attach enzymes to MWNTs, 100 mg of the as-received MWNTs (diameter 20–40 nm) (Cheap Tubes) were first 'cut' and oxidized by sonicating in 400 ml of a mixture of concentrated sulphuric and nitric acids (3:1) for 3 h. The suspension was washed with milliQ water several times by filtering through a 0.8 μm polycarbonate membrane (Millipore). Nanotubes were lyophilized and stored as a dry powder, which could be re-solubilized in water with ~ 2 min sonication. Iron and nickel were not detected when the oxidized MWNTs were characterized by X-ray photoelectron spectroscopy (Anderson materials evaluation); the detection limits for iron and nickel were 0.09 wt% and 0.05 wt%, respectively. Enzymes were attached to the oxidized MWNTs using carbodiimide chemistry as described previously²⁷.

To attach the $[\text{PA}_{63}]_7$ -binding peptide, mono-N-t-boc-amido-dPEG₁₁-amine (Quanta Biodesign) was first attached to oxidized MWNTs using carbodiimide chemistry²⁷. Following removal of the t-boc-protecting group by treatment with a mixture of HCl and 1,3-dioxane (1:3), the resulting free amines were chloroacetylated by reaction overnight with a mixture of chloroacetic anhydride and triethylamine. The nanotubes were recovered by filtration, re-suspended in water, and lyophilized. To attach the peptide, 2 mg of these nanotubes were sonicated in 2 ml of anhydrous *N,N*-dimethylformamide for 10 min. Then, 3 mg of the peptide Ac-HTSTYWLDGAPC-amide (Genemed Synthesis) and 2 μl triethylamine were added to the solution and allowed to react overnight. Unreacted chloroacetyl groups were quenched with thioglycerol. The peptide-functionalized nanotubes were characterized by nuclear magnetic resonance (NMR) spectroscopy. Control thioglycerol-functionalized nanotubes were synthesized by adding thioglycerol instead of the peptide.

NIR IRRADIATION AND DETERMINING ENZYME ACTIVITY

To test the effect of NIR irradiation on the activity of nanotube–enzyme conjugates, a solution of the conjugates (in the absence or presence of quenchers of ROS) was transferred to a quartz cuvette and exposed to radiation from a

fibre-coupled diode laser (centre wavelength = 975.5 nm, operated at power 1 W out of the fibre, laser manufactured by Spectra-Physics). The distance between the focusing lens and cuvette was adjusted to allow for a spot size of ~ 1 cm diameter. While irradiating the conjugates, aliquots were removed periodically, and enzyme activity was determined using assays based on ethanol oxidation for ADH and substrate cleavage for SC (Sigma). ADH (Sigma) catalyses the oxidation of ethanol to acetaldehyde in the presence of β -nicotinamide adenine dinucleotide (NAD), which is reduced to NADH and can be detected at 340 nm. SC catalyses the hydrolytic cleavage of the substrate, *N*-succinyl-Ala-Ala-Pro-Phe-*p*-nitroanilide (Sigma), releasing the chromophore *p*-nitroaniline, which absorbs at 405 nm. Activity was determined by measuring the increase in absorbance of the reaction mixture at the appropriate wavelength (340 or 405 nm) as a function of time.

MAKING TRANSPARENT NANOTUBE FILMS

The transparent films were fabricated as described previously²⁴. Briefly, 0.04 mg of oxidized MWNTs were sonicated in 20 ml of 1% sodium dodecyl sulphate (SDS) solution for 30 min. The solution was filtered through a 0.45 μm mixed cellulose ester membrane (Millipore) and the surfactant washed away with deionized water. The nanotube film was dried under vacuum for 30 min. The membrane was dissolved away in acetone²⁴, and the film was transferred onto a glass cover slip, dried for 30 min in air, and peeled off to give a free-standing transparent film.

CHARACTERIZING SELF-CLEANING OF FILMS BY GEL ELECTROPHORESIS

The removal of adsorbed protein by irradiation of the nanotube films was confirmed by SDS-PAGE. Transparent carbon nanotube films were formed as described above. The films were incubated with a 1 mg ml⁻¹ solution of BSA in deionized water for 30 min. Excess unadsorbed BSA was removed by washing the films with deionized water. The films were then irradiated with NIR or visible light for different intervals of time. NIR irradiation was carried out by exposure to radiation from a fibre-coupled diode laser in a quartz cuvette as previously described. Visible light irradiation experiments were carried out using a 350 W compact fluorescent bulb (SL85/65K, Sunlite), which had an output spectrum designed to mimic daylight. After adsorption of BSA, the nanotube films were incubated in water in the presence or absence of 200 mM mannitol, at a distance of ~ 10 cm from the light source for the prescribed amount of time. To ensure minimal heating of the solution, the samples were incubated in an ice bath.

For SDS-PAGE analysis, the protein adsorbed on the film was extracted using 200 μl of a 2% aqueous SDS solution. Then, 20 μl of the SDS extract was loaded onto a pre-cast 4–12% tris-glycine polyacrylamide gel (Invitrogen), and electrophoresis was performed. The protein was detected by silver staining.

Received 11 June 2007; accepted 22 October 2007;
published 9 December 2007.

References

- Chen, R. J. *et al.* Noncovalent functionalization of carbon nanotubes for highly specific electronic biosensors. *Proc. Natl Acad. Sci. USA* **100**, 4984–4989 (2003).
- Barone, P. W., Baik, S., Heller, D. A. & Strano, M. S. Near-infrared optical sensors based on single-walled carbon nanotubes. *Nature Mater.* **4**, 86–92 (2005).
- Bianco, A., Kostarelos, K., Partidos, C. D. & Prato, M. Biomedical applications of functionalised carbon nanotubes. *Chem. Commun.* 571–577 (2005).
- Kam, N. W. S., O'Connell, M., Wisdom, J. A. & Dai, H. Carbon nanotubes as multifunctional biological transporters and near-infrared agents for selective cancer cell destruction. *Proc. Natl Acad. Sci. USA* **102**, 11600–11605 (2005).
- Liu, Z. *et al.* *In vivo* biodistribution and highly efficient tumour targeting of carbon nanotubes in mice. *Nature Nanotech.* **2**, 47–52 (2006).
- Hirsch, L. R. *et al.* Nanoshell-mediated near-infrared thermal therapy of tumors under magnetic resonance guidance. *Proc. Natl Acad. Sci. USA* **11**, 13549–13554 (2003).
- Zheng, M. & Rostovtsev, V. V. Photoinduced charge transfer mediated by DNA-wrapped carbon nanotubes. *J. Am. Chem. Soc.* **128**, 7702–7703 (2006).
- Bosi, S., Da Ros, T., Spalluto, G. & Prato, M. Fullerene derivatives: an attractive tool for biological applications. *Eur. J. Med. Chem.* **38**, 913–923 (2003).
- Yamakoshi, Y. *et al.* Active oxygen species generated from photoexcited fullerene (C60) as potential medicines: O₂⁻ versus ¹O₂. *J. Am. Chem. Soc.* **125**, 12803–12809 (2003).
- Bakalova, R. *et al.* Quantum dot anti-CD conjugates: Are they potential photosensitizers or potentiators of classical photosensitizing agents in photodynamic therapy of cancer? *Nano Lett.* **4**, 1567–1573 (2004).
- Bakalova, R., Ohba, H., Zhelev, Z., Ishikawa, M. & Baba, Y. Quantum dots as photosensitizers? *Nature Biotechnol.* **22**, 1360–1361 (2004).
- Kebinski, P., Cahill, D. G., Bodapati, A., Sullivan, C. R. & Taton, T. A. Limits of localized heating by electromagnetically excited nanoparticles. *J. Appl. Phys.* **100**, 54305 (2006).
- Bulina, M. E. *et al.* A genetically encoded photosensitizer. *Nature Biotechnol.* **24**, 95–99 (2006).
- Davies, K. J. A. Protein damage and degradation by oxygen radicals. *J. Biol. Chem.* **262**, 9895–9901 (1987).
- Izumi, I., Fan, F.-R. F. & Bard, A. J. Heterogeneous photocatalytic decomposition of benzoic acid and adipic acid on platinumized TiO₂ powder. The photo-Kolbe decarboxylative route to the breakdown of the benzene ring and to the production of butane. *J. Phys. Chem.* **85**, 218–223 (1981).

16. Dukovic, G. *et al.* Reversible surface oxidation and efficient luminescence quenching in semiconductor single-wall carbon nanotubes. *J. Am. Chem. Soc.* **126**, 15269–15276 (2004).
17. Strano, M. S. *et al.* Reversible, band-gap-selective protonation of single-walled carbon nanotubes in solution. *J. Phys. Chem. B* **107**, 6979–6985 (2003).
18. Koppenol, W. H. & Butler, J. Energetics of interconversion of oxyradicals. *Adv. Free Radic. Biol. Medic.* **1**, 81–131 (1985).
19. Okazaki, K., Nakato, Y. & Murakoshi, K. Absolute potential of the Fermi level of isolated single-walled carbon nanotubes. *Phys. Rev. B* **68**, 035434 (2003).
20. Zheng, M. & Diner, B. A. Solution redox chemistry of carbon nanotubes. *J. Am. Chem. Soc.* **126**, 15490–15496 (2004).
21. Bottini, M. *et al.* Full-length single-walled carbon nanotubes decorated with streptavidin-conjugated quantum dots as multivalent intracellular fluorescent nanoprobe. *Biomacromolecules* **7**, 2259–2263 (2006).
22. Gu, L. *et al.* Single-walled carbon nanotubes displaying multivalent ligands for capturing pathogens. *Chem. Commun.* 874–876 (2005).
23. Rai, P. *et al.* Statistical pattern matching facilitates the design of polyvalent inhibitors of anthrax and cholera toxins. *Nature Biotechnol.* **24**, 582–586 (2006).
24. Wu, Z. *et al.* Transparent, conductive carbon nanotube films. *Science* **305**, 1273–1276 (2004).
25. Parkin, I. P. & Palgrave, R. G. Self-cleaning coatings. *J. Mater. Chem.* **15**, 1689–1695 (2005).
26. Karajanagi, S. S., Vertegel, A. A., Kane, R. S. & Dordick, J. S. Structure and function of enzymes adsorbed onto single-walled carbon nanotubes. *Langmuir* **20**, 11594–11599 (2004).
27. Asuri, P. *et al.* Water-soluble carbon nanotube–enzyme conjugates as functional biocatalytic formulations. *Biotech. Bioeng.* **95**, 804–811 (2006).

Acknowledgements

We acknowledge support from the National Institutes of Health (U01 AI056546) and the National Science Foundation (DMR 0642573, CBET 0348613). We also thank R. Planty for assistance with the X-ray photoelectron spectroscopy measurements.

Correspondence and requests for materials should be addressed to R.S.K.

Supplementary information accompanies the paper on www.nature.com/naturenanotechnology.

Author contributions

A.J. and S.P. designed and performed the experiments, analysed the data, and co-wrote the manuscript. S.S.B. and H.Y. carried out TEM imaging. T.B.-T. designed the experiments. R.S.K. conceived and designed the experiments, analysed the data and wrote the manuscript. All authors discussed the results and commented on the manuscript.

Reprints and permission information is available online at <http://npg.nature.com/reprintsandpermissions/>